Extended Abstracts of the 2016 International Conference on Solid State Devices and Materials, Tsukuba, 2016, pp487-488

K-3-04

Thermal Change in Resonance Wavelength of Si Resonator Sensors on Si on Insulator Substrate and Solution by Differential Operation

Amrita Kumar Sana, Shuhei Yokoyama, Yuto Nakashima, Yoshiteru Amemiya, and Shin Yokoyama

Research Institute for Nanodevice and Bio Systems, Hiroshima University
1-4-2 Kagamiyama, Higashihiroshima, Hiroshima 739-8527, Japan
Phone: +81-82-424-6265, FAX: +81-82-424-3499, E-mail: yokoyama-shin@hiroshima-u.ac.jp

Abstract

In this paper, we describe the mechanism and solution for dominating the temperature effects on refractive index based biosensing. We used differential silicon ring resonator that shows the temperature independent resonance wavelength shift.

1. Introduction

It has been known that that the refractive index of silicon greatly changes with temperature increase (see Fig. 1) [1, 2]. Silicon based biosensor where refractive index (RI) changes and is considered the sensing parameter should care about the temperature effects because it enhances the resonance wavelength shift. As the temperature changes, the device mechanical deformations happen together with the refractive index change of Si. In this work, the resonance wavelength shift of Si ring and photonic crystal resonators were investigated. In order to solve the temperature instability we proposed a differential operation of two resonators [3], where a π phase shifter is installed in one of the two outputs before merging. In this case the integral intensity of the differential output becomes temperature independent because the resonance wavelengths of both two resonators shift in parallel. The schematic structure of differential Si ring resonator and photonic crystal (PhC) based cavity type resonators [4] are shown in Figs. 2(a) and 2(b) respectively.

2. Simulation of Temperature Dependence of Resonance Wavelength Shift

Resonance wavelength shift of the resonator by temperature change is given by the following equation:

$$\Delta\lambda_{res} = \frac{\Delta n}{n}\lambda_{res} + \frac{\Delta L}{L}\lambda_{res}, \qquad (1)$$

where λ_{res}, n and L are the resonance wavelength, effective refractive index and size of the resonator respectively. $\Delta\lambda_{res}$, Δn and ΔL are the change in resonance wavelength due to the temperature change. This equation is easily derived from the equation of $\lambda_{res}= nL/m$, where m denotes the integer. As the temperature increases, Si and SiO_2 thermally expand with different thermal expansion coefficients and the silicon on insulator (SOI) substrate has a curvature shape as shown in Fig. 3. The radius of the curvature of the SOI substrate is given by the following equation [5]:

$$\frac{1}{R} = \frac{6(\alpha_1 - \alpha_2)\Delta T(1+p)^2}{h\left[3(1+p)^2 + (1+pq)(p^2 + \frac{1}{pq})\right]}, \qquad (2)$$

where h, α_1 *and* α_2 are the total thickness and thermal expansion coefficient of Si and SiO_2, p is the ratio of SiO_2 and Si thickness, q is the ratio between Young`s modulus, and ΔT is the temperature change. The change in resonator size is expressed as

$$\Delta L = \frac{dL}{2R}, \qquad (3)$$

where d is the thickness of SOI substrate.

3. Sample Fabrication

The proposed devices were fabricated using with the SiO_2 mask. Patterns of waveguides, ring and PhC resonators were made by electron beam lithography (EB), reactive ion etching (RIE) of hard-mask with CF_4 and inductively couple plasma (ICP) etching of Si with Cl_2 gas. Measurements were carried out using an infrared tunable semiconductor laser (1280~1320 nm) and an InGaAs photodetector. The scanning electron micrographs of the fabricated samples are shown in Figs. 4(a) and 4(b).

4. Results and Discussion

The temperature dependence of the differential Si ring and PhC cavity resonators are shown in Figs. 5 and 6 respectively. In Fig. 7 the measured results for the differential Si ring resonators at different temperature are shown together with the simulation results obtained by the method described in Sect. 2. It is found that the measured data well fits to the simulation result and the mechanical deformation effect is negligible ($\Delta\lambda_{res}/\Delta T$~$10^{-4}$nm/°C). The result for the PhC resonator is also shown in Fig. 8, and the same conclusion as for the ring resonator is derived. Finally the temperature stability of the differential resonator sensor is discussed. In Fig. 9 the integrated differential output for the Si ring resonators with different top cladding layer are plotted. In the differential detection, only the integrated output intensity is counted, which corresponds to the difference between the resonance wavelength shifts of two rings. And the spectral shift of the differential output is not counted. Theoretically, the integrated differential output is constant irrespective of the temperature change because the resonance curves of both two resonators shift in parallel. This is experimentally demonstrated in Fig. 9, where the changes in integrated differential outputs for the differential Si ring resonators with different top cladding layers in the temperature range from 25°C to 29°C are plotted. The data deviation due to the temperature change is within the measured scattering error (reproducibility at the same condition). This suggests that the above temperature independence of the differential operation is right.

5. Conclusion

In conclusion, the temperature effects on Si based biosensor are described in this paper. The temperature effects on resonance wavelength shift and device mechanical deformation also explain in this work.

Acknowledgement

This work was supported by a Grant-in-Aid for Scientific Research (B) (246360136, 2012) from the Ministry of Education, Culture, Sports, Science and Technology of Japan.

References
[1] G. E. Jellison *et.al.*, J. Appl. Phys. **60**, 841 (1986).
[2] J. A. Macaaulley *et.al.*, Phys. Rev. B **49**, 7408 (1994).
[3] T. Taniguchi *et al.*, Jpn. J. Appl. Phys. **55**, 04EM04 (2016).
[4] A. K. Sana *et al.*, Jpn. J. Appl. Phys. **55**, 04EM11 (2016).
[5] S. D. Brotherton *et.al.*, Solid-state Elec. **16**, 1367 (1973).

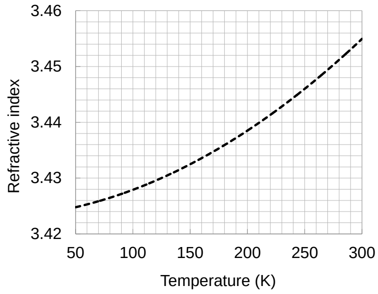

Fig. 1 Temperature effects on Si refractive index change [1].

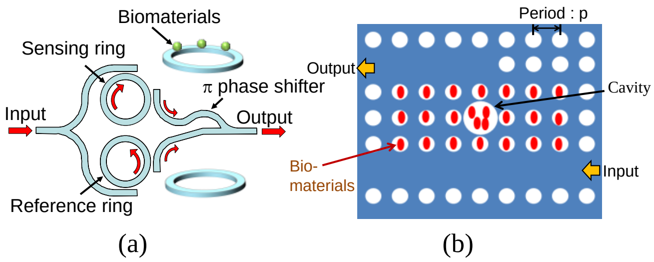

Fig. 2 Schematic of (a) differential Si ring resonator and (b) photonic crystal cavity resonator.

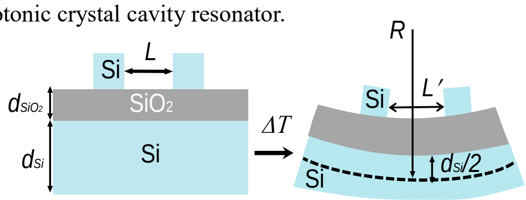

Fig. 3 Resonators shape change with temperature change.

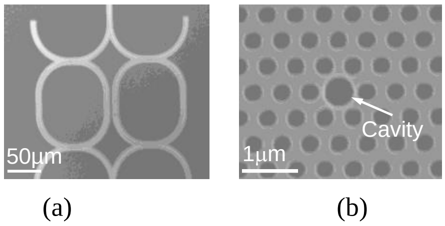

Fig. 4 Scanning electron micrograph of the fabricated devices (a) differential Si ring resonator and (b) photonic crystal cavity resonator.

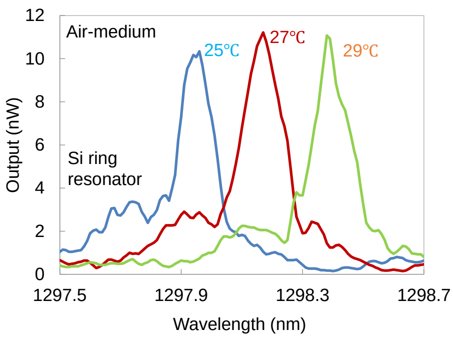

Fig. 5 Measurement results of differential Si ring resonator at different temperatures. Top cladding layer is air.

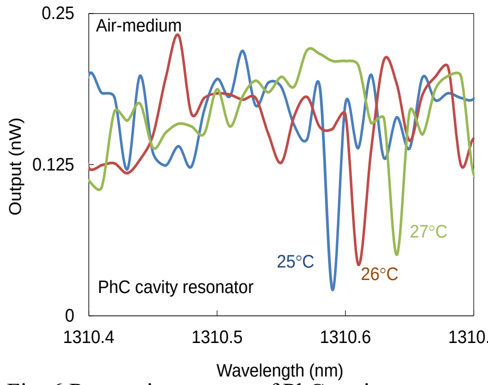

Fig. 6 Resonation spectra of PhC cavity resonator at various temperatures.

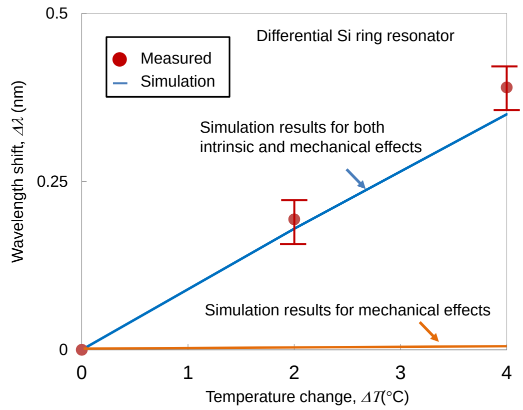

Fig. 7 Effect of temperature on resonance wavelength shift (Si ring resonator).

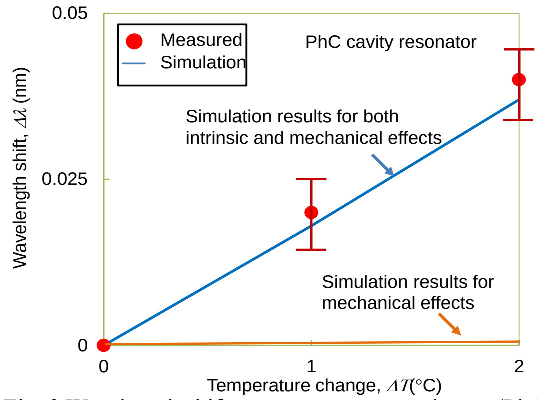

Fig. 8 Wavelength shift versus temperature change (PhC cavity resonator).

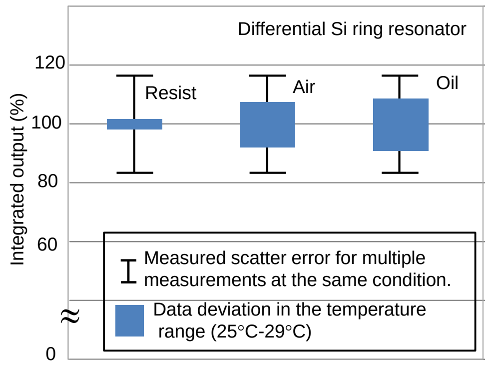

Fig. 9 Comparison of integrated light output variation in different medium at temperature range between 25°C and 29°C.